

Rapid determination of oyster lifespans and growth rates using LA-ICP-MS line scans of shell Mg/Ca ratios



Stephen R. Durham^{a,*}, David P. Gillikin^b, David H. Goodwin^c, Gregory P. Dietl^{a,d}

^a Department of Earth and Atmospheric Sciences, Cornell University, 112 Hollister Drive, Ithaca, NY 14853, USA

^b Department of Geology, Union College, 807 Union Street, Schenectady, NY 12308, USA

^c Department of Geosciences, Denison University, 100 West College Street, Granville, OH 43023, USA

^d Paleontological Research Institution, 1259 Trumansburg Road, Ithaca, NY 14850, USA

ARTICLE INFO

Article history:

Received 17 January 2017

Received in revised form 13 June 2017

Accepted 13 June 2017

Available online 17 June 2017

Keywords:

Laser ablation

Life history

Mg/Ca

Oysters

Sclerochronology

Stable oxygen isotopes

ABSTRACT

Retrospective estimates of life-history traits (e.g., growth rate, lifespan, phenology) of mollusks are valuable data for a number of fields, including paleontology, archaeology, and fisheries science. The best option for obtaining these data for species such as oysters that lack reliable morphological indicators of annual accretionary growth (e.g., growth lines) is to use time consuming and expensive stable isotope analyses. However, laser ablation analyses of Mg/Ca are faster and less expensive than stable isotope analyses, and although several studies have shown Mg/Ca ratios in bivalve shells do not reflect water temperature, there is often a weak correlation that may allow annual cycles to be detected. Here, we explore the utility of line scan analyses of Mg/Ca ratios using laser ablation-inductively coupled plasma-mass spectrometry (LA-ICP-MS) as a more rapid and less expensive method for obtaining ontogenetic age estimates of mollusk shells than more traditional oxygen stable isotope analyses. We tested this method by measuring Mg/Ca ratios from 21 fossil and modern specimens of two oyster species, *Crassostrea virginica* and *Magallana gigas* (formerly *Crassostrea gigas*), collected across a wide geographic area along the coast of the United States. We compared Mg/Ca growth profiles with either known lifespans or with growth characteristics estimated from $\delta^{18}\text{O}$ profiles. These analyses showed that Mg/Ca profiles from laser ablation analyses reliably reproduced the annual features of the more widely used $\delta^{18}\text{O}$ profiles. In total, 97% ($n = 102$) of all seasonal peaks and troughs, including both those from the $\delta^{18}\text{O}$ profiles and the expected patterns in the shells of known age, were detectable in the Mg/Ca profiles. We conclude that laser ablation analysis of Mg/Ca ratios is a rapid and cost effective alternative to stable isotope analysis for retrospective estimation of the growth characteristics of oysters and potentially other taxa with shells lacking reliable annual morphological features.

© 2017 Elsevier B.V. All rights reserved.

1. Introduction

Determination of life-history traits (e.g., growth rate, lifespan, phenology) of mollusks is an important task for researchers in a number of fields, including paleontology, archaeology, fisheries science, and marine biology for myriad research purposes, such as studies of species' responses to environmental change and evaluations of the fishing behaviors of past human populations (Kirby et al., 1998; Andrus and Crowe, 2000; Kirby, 2001; Mann et al., 2009; Harding et al., 2010; Lartaud et al., 2010; Andrus, 2011; Thomas, 2015; Rick et al., 2016; Savarese et al., 2016; Twaddle et al., 2016). This information is usually gathered by analyzing shells or parts of shells exhibiting regular accretionary growth, the characteristics of which often display seasonal

periodicities. For instance, shell growth rates and lifespans of the venerid clam *Mercenaria mercenaria* can be estimated by counting growth bands in polished shell cross-sections under a microscope (e.g., Jones et al., 1989). However, determination of life-history traits from the shells of other mollusk groups that in many cases lack simple-to-interpret morphological features, such as oysters, is more challenging.

A variety of methods has been used to estimate the growth characteristics of oyster shells retrospectively, such as tracking cohorts using population size-frequency distributions (e.g., Mann et al., 2009), counting growth lines or undulations of the surface of the resilifer (hinge plate) of left valves (Custer and Doms, 1990; Richardson et al., 1993; Kirby et al., 1998; Johnson et al., 2007; Kraeuter et al., 2007; Fan et al., 2011; Savarese et al., 2016), cathodoluminescence imaging to reveal seasonal Mn^{2+} variations (Langlet et al., 2006; Lartaud et al., 2010), and sclerochemical analyses (sensu Gröcke and Gillikin, 2008) of stable isotopes or trace elements in the shell (e.g., Kirby et al., 1998; Surge and

* Corresponding author.

E-mail addresses: srd77@cornell.edu (S.R. Durham), gillikid@union.edu (D.P. Gillikin), goodwind@denison.edu (D.H. Goodwin), gpd3@cornell.edu (G.P. Dietl).

Lohmann, 2008; Goodwin et al., 2010, 2013; Fan et al., 2011; Bougeois et al., 2014). Although some studies have found that morphological features of oyster shells, such as growth lines or undulations on the surface of the resilifer, are annual (e.g., Kirby et al., 1998; Kraeuter et al., 2007; Fan et al., 2011), others have found that estimation of oyster growth characteristics from such features is inaccurate (e.g., Hong et al., 1995; Andrus and Crowe, 2000; Surge et al., 2001). By contrast, geochemical analyses are arguably the most accurate and reliable methods of retrospective age determination, but can be expensive and time consuming. For instance, the $^{18}\text{O}:^{16}\text{O}$ ratio in shell carbonate, expressed as $\delta^{18}\text{O}$ values, is a common and trusted method of estimating a wide range of growth-related characteristics from mollusk shells (e.g., size-at-age relationships, lifespan, growth rate, and season of recruitment or death), including oysters (Kirby et al., 1998; Goodwin et al., 2010, 2013). Stable oxygen isotope analysis, however, often requires hours of sample collection followed by a lengthy analysis procedure (or weeks of waiting for results if the samples are sent to a commercial lab) and analyzing large numbers of specimens is usually cost-prohibitive.

An alternative geochemical proxy, whose applications to assessing mollusk growth characteristics have yet to be widely explored, is the magnesium to calcium (Mg/Ca) ratio in shell carbonate. The Mg/Ca ratio of biogenic minerals has been intensely studied as a temperature proxy in a variety of calcifying taxa (e.g., sponges: Swart et al., 2002; Fabre and Lathuiliere, 2007; corals: Watanabe et al., 2001; Sherwood et al., 2005; and mollusks: Dodd, 1965; Klein et al., 1996; Vander Putten et al., 1999; Wanamaker et al., 2008; Freitas et al., 2012), including oysters (Surge and Lohmann, 2008; Mouchi et al., 2013; Bougeois et al., 2014, 2016; Tynan et al., 2017). Although evidence shows that Mg/Ca ratios are not reliable paleothermometers in the case of mollusks due to vital effects associated with Mg^{2+} incorporation into shell carbonate (coefficient of determination typically <0.5 ; e.g., Lorrain et al., 2005; Wanamaker et al., 2008; Surge and Lohmann, 2008; Poulain et al., 2015; Graniero et al., 2017), the sensitivity of Mg/Ca ratios to seasonally correlated environmental forcings or shell microstructural patterns (e.g., Marali et al., 2017) may be sufficient as an alternative to $\delta^{18}\text{O}$ values for estimation of growth characteristics such as lifespan and growth rate (e.g., Richardson et al., 2004, 2005; Bougeois et al., 2014; but see Graniero et al., 2017).

The major potential advantage of using Mg/Ca ratios for estimating growth characteristics is that they can be analyzed more rapidly and are less expensive than $\delta^{18}\text{O}$ analyses. Mg/Ca ratios are most often measured using laser ablation-inductively coupled plasma-mass spectrometry (LA-ICP-MS). This technique uses one of several kinds of lasers to ablate small amounts of shell that are then swept into an ICP-MS by a stream of helium and/or argon (Durrant and Ward, 2005). Trace element concentrations are measured in real time and, depending on the scan speed and specimen size, entire specimens can be analyzed in minutes. Our experiences suggest that around 10–15 specimens can be analyzed in one day by LA-ICP-MS, and per-specimen costs are currently approximately 1/10 those of stable isotope analysis.

Here, we test Mg/Ca ratios measured from LA-ICP-MS line scans as a rapid and cost-effective method of estimating growth characteristics of oysters. We used the eastern oyster, *Crassostrea virginica*, because they lack reliable morphological indicators of annual accretionary growth (e.g., distinct annual growth lines; Hong et al., 1995; Andrus and Crowe, 2000; Surge et al., 2001), leaving few alternatives to sclerochemical approaches for obtaining accurate retrospective estimates of life-history traits from their shells. Oysters are also a group for which growth data are frequently needed—information on growth rates and population dynamics of *C. virginica*, mostly gathered from cohort analyses using size-frequency distributions, is important for the conservation, restoration, and management of oyster populations (e.g., Harding et al., 2010; Levinton et al., 2013; Baggett et al., 2015). Accurate estimates of oyster lifespans and growth rates from geochemical analyses of shells could complement these data by, for instance, allowing verification of cohort identifications and making rapid and

inexpensive investigations of growth characteristics in the past possible through retrospective analysis of dead shells.

2. Material and methods

Sixteen *C. virginica* specimens were analyzed for both Mg/Ca ratios and $\delta^{18}\text{O}$ values: one live-collected specimen from Connecticut; one live-collected specimen and six modern dead-collected shells from South Carolina; seven fossil shells from the Pleistocene Canepatch Formation in South Carolina; and one modern dead-collected specimen from Louisiana (Table 1). Additionally, Mg/Ca was analyzed from three hatchery-reared specimens of known age (nine months; Dec. to Aug.) from North Carolina (Table 1). Together, these specimens represent wide geographic and temporal range, including most of the North American portion of *C. virginica*'s geographic range (Gulf of St. Lawrence to the Gulf of Mexico; Carriker and Gaffney, 1996) and approximately 350,000 years of geological history. We also tested the method on two specimens of *Magallana gigas* (formerly *Crassostrea gigas*, see Salvi and Mariottini, 2016), collected from San Francisco Bay in California, in order to examine the utility of Mg/Ca profiles in a different oyster taxon, as well as the performance of the method in a location with lower-amplitude seasonal temperature variability (Fig. 1). Stable isotope and LA-ICP-MS analyses for the California specimens were performed as part of previous work by a subset of the authors, but the Mg/Ca data were not previously reported (see Goodwin et al., 2010, 2013 for details). Thus, our analysis was designed to incorporate environmental and geographic variability, representing coastal intertidal marsh environments with a variety of seasonal patterns in temperature (Fig. 1) from four different ecoregions (Virginian, Carolinian, Northern Gulf of Mexico, and Northern California; sensu Spalding et al., 2007).

We followed Goodwin et al. (2010, 2013) in analyzing cross-sections of the hinge plate (resilifer) of the left valve for each specimen (Fig. 2). All specimens were prepared by cutting a cross-section through the resilifer parallel to the direction of growth and perpendicular to the anteroposterior axis with a low-speed diamond saw (Fig. 2a). One of the resilifer halves of each specimen was then polished using a series of fine-grit silicon carbide sandpapers (up to P4000 grit) and mounted on a glass slide such that the polished cross-section was horizontal and level.

Following O'Neil and Gillikin (2014), each specimen was analyzed for Mg/Ca ratios by ablating overlapping line patterns along the foliated calcite layer of each resilifer (avoiding the alternating chalky and foliated calcite mineralogy that characterizes the umbonal cavity), parallel to the direction of growth (Fig. 2c), with a CETAC LSX-213 frequency quintupled Nd:YAG laser ablation unit ($\lambda = 213$ nm) connected to a Perkin Elmer Elan 6100 ICP-MS at Union College in Schenectady, New York. A 50 μm spot size was used with a shot frequency of 10 Hz. Each line was pre-ablated at a scan rate of 150 $\mu\text{m}/\text{s}$ to remove contaminants before being scanned again at a scan rate of 50 $\mu\text{m}/\text{s}$, resulting in an approximate sampling resolution of 50 μm . For all line scans, a 15 s shutter delay was used so that each series of sample data was preceded by gas blank data. The gas blank values were subtracted from the sample values in order to remove the gas signal from the specimen data. ^{43}Ca was used as an internal standard and all Mg/Ca intensity values were calibrated using the United States Geological Survey MACS-3 carbonate standard¹ (values from USGS, 2012). The average calibrated MACS-3 Mg concentration had a relative standard deviation (%RSD) of 2.4% ($n = 32$ over eight analytical days), showing excellent precision. The calibration was checked using the non-matrix-matched NIST 610 glass standard, yielding an average Mg concentration of 445 ± 20 ppm—within 5% of the recommended value (465 ppm; Pearce et al., 1997)—and 4.5%RSD

¹ Although we present our data in molar units to allow comparison with other studies, this step is not necessary to estimate growth characteristics from the Mg/Ca profiles; ratios of blank-subtracted raw counts of Mg and Ca (i.e., units of counts/counts) are generally sufficient for these analyses.

Table 1
Information on the specimens used in the study.

Species	Collection location	Collection type	Specimen ID	Collection date	Mg/Ca evaluation	Resiliifer height (mm)	Resiliifer width (mm)	Valve height (mm)	Valve width (mm)	n ($\delta^{18}\text{O}$, $\delta^{13}\text{C}$)	n (Mg/Ca)	Mean $\delta^{18}\text{O}$ (VPDB)	SD $\delta^{18}\text{O}$ (VPDB)	Mean $\delta^{13}\text{C}$ (VPDB)	SD $\delta^{13}\text{C}$ (VPDB)	Mean Mg/Ca (mmol/mol)	SD Mg/Ca (mmol/mol)
<i>Crassostrea virginica</i>	Madison, Connecticut	Live	CT-L-01	9/6/2014	$\delta^{18}\text{O}$, $\delta^{13}\text{C}$	29	37	177	89	36	1326	-2.71	0.81	-1.51	0.27	1.91	0.61
		Dead	LA-D-01	1/25/2013	$\delta^{18}\text{O}$, $\delta^{13}\text{C}$	10	13	64	38	13	225	-2.65	0.95	-3.05	0.72	2.71	1.14
	Grand Terre Island, Louisiana	Dead	SC-D-01	2/20/2014	$\delta^{18}\text{O}$, $\delta^{13}\text{C}$	23	16	118	36	40	494	-1.41	1.01	-1.73	0.69	2.31	0.69
		Dead	SC-D-02	2/20/2014	$\delta^{18}\text{O}$, $\delta^{13}\text{C}$	13	13	59	29	15	274	-1.42	0.98	-2.11	0.42	2.44	0.80
	Watie's Island, South Carolina	Dead	SC-D-03	2/20/2014	$\delta^{18}\text{O}$, $\delta^{13}\text{C}$	27	14	120	28	38	648	-1.75	1.12	-2.05	0.51	3.01	0.93
		Dead	SC-D-04	5/16/2015	$\delta^{18}\text{O}$, $\delta^{13}\text{C}$	37	22	127	48	38	905	-0.44	1.19	-0.94	0.27	2.90	0.89
		Dead	SC-D-05	5/16/2015	$\delta^{18}\text{O}$, $\delta^{13}\text{C}$	31	21	92	41	41	705	-0.50	1.07	-0.99	0.27	2.52	0.75
		Dead	SC-D-06	7/20/2013	$\delta^{18}\text{O}$, $\delta^{13}\text{C}$	14	12	63	28	20	352	-0.42	0.72	-1.12	0.29	1.53	0.62
	North Myrtle Beach, South Carolina	Fossil	SC-F-01	7/20/2013	$\delta^{18}\text{O}$, $\delta^{13}\text{C}$	14	10	61	24	18	328	-0.24	1.12	-0.45	0.81	2.00	0.47
		Fossil	SC-F-02	7/20/2013	$\delta^{18}\text{O}$, $\delta^{13}\text{C}$	28	15	111	31	37	634	-0.64	0.93	0.15	0.62	2.15	0.51
Fossil		SC-F-03	7/21/2013	$\delta^{18}\text{O}$, $\delta^{13}\text{C}$	22	16	127	41	30	529	-0.34	1.14	-0.48	0.54	3.00	0.92	
Fossil		SC-F-04	7/21/2013	$\delta^{18}\text{O}$, $\delta^{13}\text{C}$	35	17	130	41	54	912	-0.07	1.22	-0.11	0.37	3.01	1.06	
Fossil		SC-F-05	7/21/2013	$\delta^{18}\text{O}$, $\delta^{13}\text{C}$	20	14	88	27	26	470	-1.03	0.98	-0.76	0.49	2.72	0.90	
Fossil		SC-F-06	7/21/2013	$\delta^{18}\text{O}$, $\delta^{13}\text{C}$	14	10	75	30	15	587	-0.64	1.16	-0.20	0.24	1.93	0.76	
Fossil		SC-F-07	7/21/2013	$\delta^{18}\text{O}$, $\delta^{13}\text{C}$	11	15	53	25	13	252	-0.36	1.06	-0.78	0.49	2.68	0.78	
Live		SC-L-01	2/20/2014	Known age	12	20	80	26	27	390	-0.71	0.90	-1.87	0.57	2.71	0.62	
Live		NC-L-01	8/7/2015	Known age	14	22	89	61	n/a	245	n/a	n/a	n/a	n/a	2.51	0.96	
Live		NC-L-02	8/7/2015	Known age	14	22	94	57	n/a	312	n/a	n/a	n/a	n/a	2.87	0.93	
Watie's Island, South Carolina	Live	CA-L-01	7/28/2006	$\delta^{18}\text{O}$, $\delta^{13}\text{C}$	14	21	88	62	n/a	250	n/a	n/a	n/a	2.88	1.23		
	Live	CA-L-02	7/28/2006	$\delta^{18}\text{O}$, $\delta^{13}\text{C}$	14	21	126	42	39	2352	-2.08	1.24	-4.79	1.04	0.80	0.21	
Jarrett Bay, North Carolina	Live	NC-L-03	8/7/2015	Known age	14	22	88	62	n/a	250	n/a	n/a	n/a	2.88	1.23		
	Live	CA-L-01	7/28/2006	$\delta^{18}\text{O}$, $\delta^{13}\text{C}$	14	21	126	42	39	2352	-2.08	1.24	-4.79	1.04	0.80	0.21	
Magallana gigas	San Francisco Bay, California	Live	CA-L-02	7/28/2006	$\delta^{18}\text{O}$, $\delta^{13}\text{C}$	14	21	71	39	45	1598	-2.01	0.93	-4.95	1.13	0.48	0.18

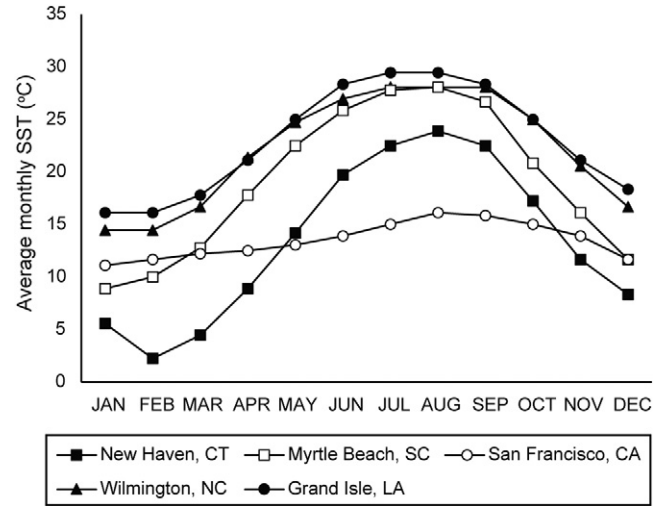


Fig. 1. Plots of average monthly temperature for areas near our sample locations. Data are from the National Oceanic and Atmospheric Administration (NOAA) Coastal Water Temperature Guide (https://www.nodc.noaa.gov/dsdt/cwtg/all_meanT.html; Accessed 11/3/2016). Data are averages of several years to decades, depending on the duration of monitoring records at each location, as reported by NOAA. CT = Connecticut; NC = North Carolina; SC = South Carolina; LA = Louisiana; CA = California.

($n = 24$ over eight analytical days). Details on the analyses and calibrations for the California specimens can be found in Goodwin et al. (2013), which were analyzed on the same LA-ICP-MS.

Each *C. virginica* resiliifer specimen, excluding the hatchery-raised individuals of known age from North Carolina, was then re-polished and a series of carbonate powder samples was drilled along the same foliated calcite layer, parallel to the direction of growth (from the umbo to the growth margin; Fig. 2b), using a Merchanteq micromill at Syracuse University in Syracuse, New York. The carbonate samples were analyzed for $\delta^{18}\text{O}$ and $\delta^{13}\text{C}$ values using a Finnigan MAT 251 coupled to a Finnigan Kiel automated preparation device at the University of Michigan's stable isotope laboratory in Ann Arbor, Michigan or a Thermo Gas Bench II connected to a Thermo Delta Advantage mass spectrometer in continuous flow mode at the stable isotope laboratory at Union College. Analyses from the University of Michigan and Union College both had an analytical uncertainty for $\delta^{18}\text{O}$ and $\delta^{13}\text{C}$ values of $<0.1\%$ (VPDB) based on 22 and 13 NBS-19 standards, respectively. Details on the $\delta^{18}\text{O}$ and $\delta^{13}\text{C}$ analyses for the California specimens can be found in Goodwin et al. (2010, 2013).

The resulting Mg/Ca and $\delta^{18}\text{O}$ and $\delta^{13}\text{C}$ profiles were matched by measuring sample distances for both the laser line scans and the micromill samples from digital photographs, using a single scale, with the ImageJ 1.51f image processing software (Rasband, 1997). Sample distances for the North Carolina hatchery specimens were estimated using the same method. The Mg/Ca, $\delta^{18}\text{O}$, and $\delta^{13}\text{C}$ values were then plotted against the sample distances from the umbo in order to compare the profiles.

To aid in distinguishing the lower-frequency annual variability from the higher-frequency intra-annual variability in the high-resolution laser ablation line-scan data, each Mg/Ca profile was centered around zero by subtracting the linear trendline values from the raw data to remove ontogenetic trends and applying running medians to the data. Linear detrending is commonly used in sclerochronology and is among the simplest detrending methods available (e.g., Cook and Holmes, 1986; Cook and Krusic, 2005), but we also tested two alternative detrending methods with variance-stabilizing properties on a subset of the Mg/Ca profiles (measured/predicted ratios and the adaptive power transformation, Cook and Peters, 1997). The choice of detrending method did not impact our interpretations of annual peaks and troughs in the test profiles (Appendix 1), so we used the simple, widely used linear detrending method. Note that detrending was inappropriate for

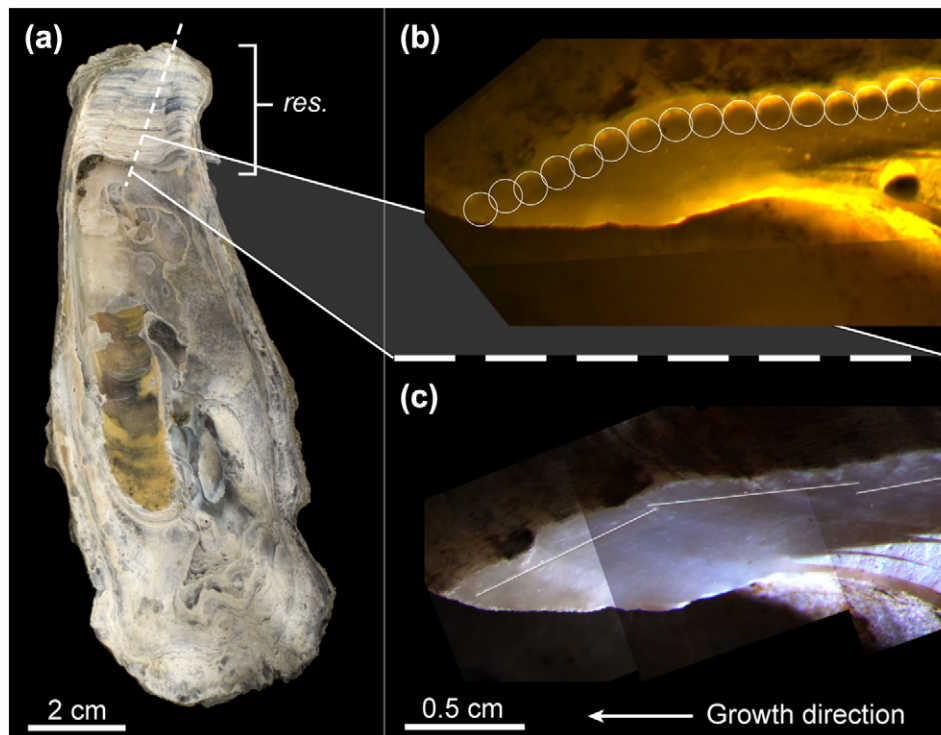


Fig. 2. (a) Images of a fossil *C. virginica* left valve highlighting the resifer (*res.*) and the plane cut to produce the cross-sections used in our geochemical analyses. The composite images on the right show the growth margin of the resifer cross-section for specimen SC-F-04. The foliated calcite layer at the resifer surface was sampled with (b) a micromill and (c) by laser ablation. Micromill point samples (b) and laser lines (c) are highlighted with circles and lines, respectively. Images for panels (b) and (c) were taken with different cameras and lighting. Note: the 0.5 cm scale bar and *growth direction* label apply to both (b) and (c).

specimens < 1 year old, because in such cases the trend lines would track intra-annual variation in Mg/Ca, obscuring the incomplete annual pattern (e.g., Fig. A3.16). Thus, the Mg/Ca profiles of the three nine-month-old North Carolina specimens were not adjusted for ontogenetic trends (Fig. A3.17).

Running medians with adaptive median windows based on oyster growth data were plotted to help distinguish annual variability in the Mg/Ca profiles from intra-annual variability. We used “adaptive” median windows because oyster growth rate slows during ontogeny—meaning more intra-annual Mg/Ca variation must be discounted in earlier parts of the profiles than in later portions. This correction was achieved by having the median windows decrease in width with increasing distance from the umbo according to regressions of oyster growth rate against specimen age (size-at-age relationships were estimated from the $\delta^{18}\text{O}$ profiles). Further, because oyster growth patterns vary with latitude (e.g., Shumway, 1996), we plotted separate medians based on growth data from three geographical and temporal subsets of our oyster specimens. The three geographic and temporal subsets were 1) the Connecticut specimen, 2) the modern South Carolina specimens, and 3) the fossil South Carolina specimens (Fig. 3). All three medians were plotted on each profile in order to test whether local oyster growth data are needed to use this method—if the same life-history interpretations were given by all three medians, this result would indicate that regional oyster growth data would be sufficient for future uses of the method. The windows for the running medians were all scaled so that a growth distance of 40 mm would result in a median window width of five data points. A fourth running median was calculated for each specimen individually—using the growth data from the live-collected South Carolina specimens—that scaled the median window widths to five data points at the maximum growth distance for each specimen. These trendlines were then compared with the $\delta^{18}\text{O}$ profiles to evaluate the ability of Mg/Ca to capture annual signals. Peaks and troughs in the $\delta^{18}\text{O}$ profiles were matched visually to the closest peak in the corresponding Mg/Ca profile based on the following criteria. A $\delta^{18}\text{O}$ peak

was considered *detectable* in the Mg/Ca profile if all running medians substantially crossed zero in the direction corresponding to the $\delta^{18}\text{O}$ peak or trough. In cases where features of the $\delta^{18}\text{O}$ profile were visible in the Mg/Ca profile, but one or more running medians did not substantially cross zero, the peak was considered *present but ambiguous*. *Undetectable* $\delta^{18}\text{O}$ peaks were those that would have been missed in the Mg/Ca profile in the absence of the $\delta^{18}\text{O}$ profiles.

3. Results and discussion

Annual peaks in the $\delta^{18}\text{O}$ profiles were identifiable in the majority of Mg/Ca profiles (See Appendix 2 for raw Mg/Ca and stable isotope

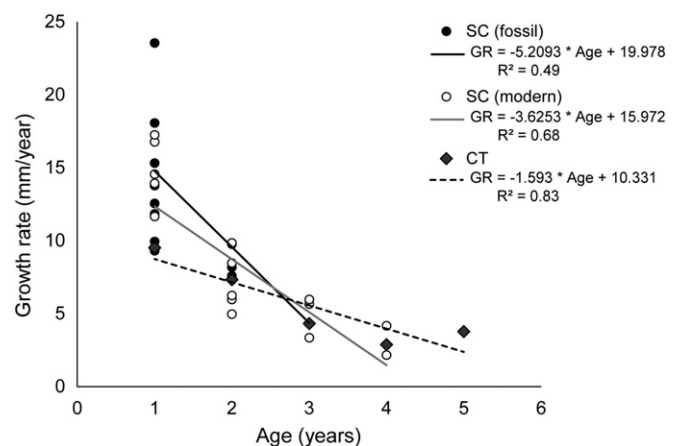


Fig. 3. Regressions of resifer growth rate (GR) against age in years for the specimen from Connecticut (CT) and modern and fossil dead specimens from South Carolina (SC; determined from $\delta^{18}\text{O}$ profiles). The regressions were used to determine the window widths of the running medians to aid in Mg/Ca profile interpretations (see text for details).

values). Further, our results agree with those of previous studies reporting that the foliated calcite growth lines in the oyster hinge cross-sections may not always form with annual periodicity (e.g., Hong et al., 1995; Andrus and Crowe, 2000; Surge et al., 2001; Fig. 4), highlighting the importance of geochemical analyses for evaluating growth characteristics in this taxonomic group. Collectively, out of 105 total peaks and troughs in the $\delta^{18}\text{O}$ profiles of the Connecticut, South Carolina, and California oyster specimens, 97% ($n = 102$) were detectable in the Mg/Ca profiles, 9% ($n = 9$) of which would have been ambiguous in the Mg/Ca profiles in the absence of the $\delta^{18}\text{O}$ profiles. Three percent ($n = 3$) of the $\delta^{18}\text{O}$ profile peaks and troughs were undetectable in the Mg/Ca profiles (see Fig. 5 for an example; profiles for all specimens can be found in Appendix 3). The specimen from

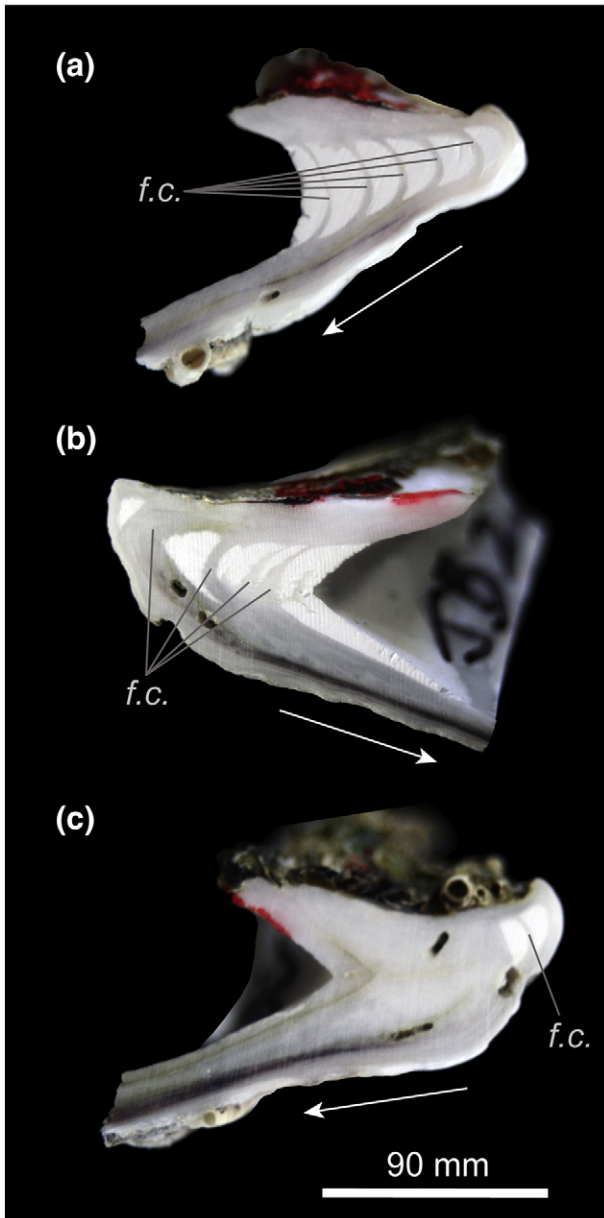


Fig. 4. Resiliifer cross-sections of the three North Carolina specimens included in our study: (a) NC-L-01, (b) NC-L-02, and (c) NC-L-03. These specimens were live-collected in August 2015 at the same time from the same hatchery at nine months of age, yet show highly variable numbers of foliated calcite growth lines (examples are labeled *f.c.*), demonstrating that the lines are not annual morphological features in these specimens. Scale bar applies to all images. White arrows indicate direction of growth.

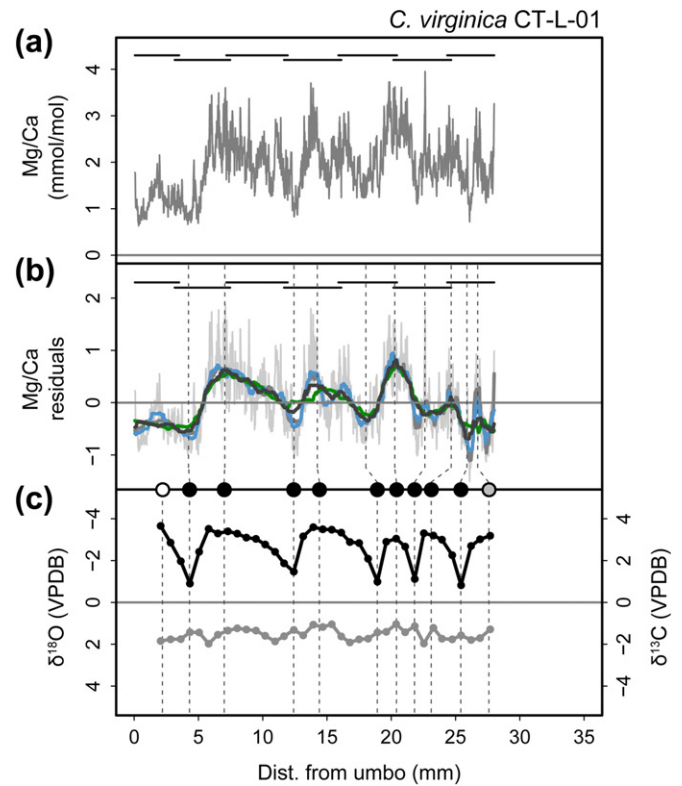


Fig. 5. Plots showing (a) the raw Mg/Ca ratio data, (b) the Mg/Ca profile centered around zero with four running medians, and (c) the $\delta^{18}\text{O}$ (black line, axis inverted) and $\delta^{13}\text{C}$ (grey line) profiles for the *C. virginica* specimen CT-L-01. Dark grey lines above the profile in panels (a) and (b) represent the distances covered by individual laser ablation line scans. Mean-subtracted data (i.e., residuals) in panel (b) are in light grey. The four running median trendlines in panel (b) have median windows based on growth rate/age relationships for: 1. the live-collected Connecticut specimen (blue); 2. the fossil South Carolina specimens (green); 3. the modern South Carolina specimens (dark grey); and 4. the modern South Carolina specimens, but with window widths scaled to the individual specimen (grey). See text for details. Vertical dashed lines that cross panels (b) and (c) correspond with peaks and troughs in the $\delta^{18}\text{O}$ profile. Shaded circles in between the two panels indicate whether the corresponding peak or trough in the $\delta^{18}\text{O}$ profile is detectable in the Mg/Ca profile (black = detectable; grey = present but ambiguous; white = undetectable).

Louisiana was not included in these totals because the geochemical results suggested it was less than a year old² (Fig. A3.16).

The Mg/Ca profiles matched all $\delta^{18}\text{O}$ peaks in nine of the 17 shells analyzed that were more than one year old, and only three specimens had $\delta^{18}\text{O}$ peaks that were undetectable in the Mg/Ca profiles (Appendix 3).³ Lifespan estimates based on each of the four medians were equal for six of the 17 specimens (35%) that were over one year old and were within one year or less of each other for 14 of the 17 specimens (82%). The medians based on Connecticut growth data and the individually scaled modern dead South Carolina data tended to overestimate the

² This conclusion was based on three factors: 1) the raw Mg/Ca profile had a prominent positive slope, similar to the nine-month-old specimens from North Carolina; 2) the only major positive excursion in the $\delta^{18}\text{O}$ profile corresponded to a large positive excursion in the $\delta^{13}\text{C}$ profile and was not visible in the Mg/Ca profile, suggesting that it may not have been a winter seasonal signal; and 3) the Louisiana specimen was from a lower latitude than the South Carolina specimens (so would likely have grown as fast or faster than them), several of which grew 10–20 mm in their first year (Appendix 3). Finally, the match between the median patterns and the $\delta^{18}\text{O}$ profile for the Louisiana specimen is poor (Fig. A3.16).

³ It should be noted that the Mg/Ca peaks and troughs were occasionally offset from the corresponding distance position of their counterparts in the $\delta^{18}\text{O}$ profiles. We consider these offsets to be related to the difference in spatial and temporal averaging between the LA-ICP-MS and stable isotope sampling methods and the fact that we matched the $\delta^{18}\text{O}$ peaks and troughs to the running median trendlines rather than the Mg/Ca profiles themselves.

corresponding $\delta^{18}\text{O}$ profile lifespan estimates, and the medians based on the growth data from fossil dead South Carolina specimens and the modern dead South Carolina data (with windows scaled to 40 mm) more frequently underestimated the corresponding $\delta^{18}\text{O}$ profile lifespan estimates. Overall, lifespan estimates based on 67 out of the 68 medians (98.5%) were within ± 1 year of the corresponding $\delta^{18}\text{O}$ profile estimates, and the average differences between Mg/Ca profile and $\delta^{18}\text{O}$ profile lifespan estimates were 0.21 ± 0.41 years, -0.18 ± 0.52 years, -0.18 ± 0.47 years, and 0.46 ± 0.81 years, for the medians based on growth data from the Connecticut specimen, the South Carolina fossil dead specimens, and the South Carolina modern dead specimens with windows scaled to 40 mm and to the maximum growth distance of each specimen, respectively. Further, the Mg/Ca profiles accurately represented the lifespans of the three nine-month-old *C. virginica* specimens from North Carolina (Fig. A3.17), and all present but ambiguous and undetectable peaks occurred at the beginning and/or end of growth profiles, areas in which the annual pattern is often not clear, even for $\delta^{18}\text{O}$ profiles (e.g., Goodwin et al., 2003). Altogether, these results suggest that Mg/Ca profiles are useful alternatives to $\delta^{18}\text{O}$ profiles for determination of growth characteristics, such as lifespan and growth rate,⁴ in oysters.

These encouraging results for oysters also suggest that this method is likely to be useful for many other molluscan taxa. The oysters studied here produce calcite shells, which are expected to incorporate Mg relatively easily due to the similar crystal structures of MgCO_3 and CaCO_3 (Oomori et al., 1987), suggesting that this method is likely to work well for analyzing the shells of other calcitic mollusk species. Further, although the Mg partition coefficient is about 100 times lower in aragonite than in calcite (Oomori et al., 1987; Poulain et al., 2015)—suggesting that there should be relatively low Mg incorporation in aragonitic mollusk shells—seasonally correlated Mg/Ca ratios have been reported for a number of aragonitic mollusk taxa (e.g., Takesue and van Geen, 2004; Richardson et al., 2005; Schöne et al., 2011; Marali et al., 2017; but see also Foster et al., 2008). The Mg/Ca ratio values reported in some of these studies are also very similar to those of the calcite shells reported here (e.g., Takesue and van Geen, 2004; Schöne et al., 2011). This similarity despite the differences in Mg/Ca ratios between inorganic aragonite and calcite is likely due to the vital effects associated with biogenic carbonates. Thus, LA-ICP-MS analysis of Mg/Ca ratios is likely applicable to a wide variety of molluscan taxa, including both aragonitic and calcitic species.

3.1. Effects of species, seasonality, geography, and growth rate on Mg/Ca profile interpretations

The age estimates from Mg/Ca profiles largely agree with those from the $\delta^{18}\text{O}$ profiles of all specimens analyzed, including both *C. virginica* and *M. gigas* and across all localities. This result demonstrates that Mg/Ca profiles can be used to estimate growth characteristics even when seasonal variability in temperature is relatively low, as is the case in San Francisco Bay (Fig. 1). Despite the overall agreement among the medians and with the corresponding $\delta^{18}\text{O}$ profiles, growth variability between specimens from different locations did influence the performance of the running medians. For instance, the growth differences between localities in our study qualitatively corresponded to expectations based on differences in temperature (Shumway, 1996): the Connecticut specimen, from our northernmost locality, grew most slowly and its growth rate decreased the least between years, and the fossil South Carolina specimens, from a lower latitude, grew most rapidly and

decreased their growth fastest with age (Fig. 3). The modern South Carolina *C. virginica* specimens were intermediate in their growth rate and the rate of decline in growth rate over ontogeny (Fig. 3). This pattern also fits with interpretations of the Pleistocene Canepatch Formation that suggest it was deposited during a warm interglacial period (although exactly which one is uncertain; e.g., Wehmiller et al., 1988).

These variations in growth characteristics were evident in the performance of the running medians because they determined the patterns of median window widths over the Mg/Ca profile distances. For instance, because the Connecticut specimen grew relatively slowly and had a relatively small decrease in growth rate over time, the median windows based on this relationship were narrow and did not change very much with shell distance. The result was an increased sensitivity in this running median to intra-annual variation in the Mg/Ca profiles for specimens from warmer locations (e.g., South Carolina) that had a greater difference in growth rate between early and late ontogeny (Fig. 6). The opposite was true of the running median based on growth of the fossil South Carolina specimens, which showed the most rapid growth early in ontogeny and the steepest decline in growth rate with time (Fig. 3). This running median tended to have windows that began very wide and narrowed rapidly with shell distance, which sometimes resulted in insensitivity to inter-annual variability in the Mg/Ca profiles, especially the ontogenetically early sections (Fig. 6).

The variability in patterns of growth rate also affected the performance of the running median scaled for each specimen individually versus the one scaled to 40 mm growth distance. Interestingly, the individually scaled median often matched the running median based on the Connecticut specimen growth characteristics fairly closely because they both tended to have relatively narrow median windows (though in the former the narrow windows were the result of scaling to shorter shell distances, whereas the latter had narrow windows because of the slow growth rate of the Connecticut specimen). Although this sensitivity made both medians, especially the individually scaled median, susceptible to overestimating the $\delta^{18}\text{O}$ profile lifespan estimates (e.g., Figs. A3.13–15), in other cases they captured important variation towards the ends of the Mg/Ca profiles that was missed by the other medians (e.g., Figs. A3.1, A3.2, A3.5). Thus, basing our interpretations of oyster lifespans from the Mg/Ca data on multiple running medians helped account for the effects of geographic and environmental variations in growth.

3.2. Sources of variation between Mg/Ca and $\delta^{18}\text{O}$ profiles

Potential sources of variation between the Mg/Ca and $\delta^{18}\text{O}$ profiles could include variation in insoluble organic matrix content of the shell with growth rate, differential effects of salinity variations on the Mg/Ca and $\delta^{18}\text{O}$ profiles, and the distance of the samples from the edge of the resiliifer cross-section. For instance, it has been shown that the concentration of insoluble organic matrix (IOM) increases at growth lines in the aragonitic bivalve *Arctica islandica* (i.e., when shell growth slows; Schöne et al., 2010), leading to errors in the measured Mg/Ca ratios by LA-ICP-MS. This variation in IOM concentration could effectively decrease the amplitude of seasonal variation in Mg/Ca profiles. For instance, growth lines in bivalve shells are often produced during winter months at mid to high latitudes, which tend to be characterized by low Mg/Ca ratios in the shell, but the increased concentrations of Mg-enriched IOM at these growth lines might dampen that pattern. Thus, if such heterogeneous distribution of IOM is also characteristic of the oysters analyzed here, then this effect could contribute to difficulties in interpreting some annual cycles in the Mg/Ca profiles in our study by decreasing the amplitude of annual cycles relative to the often noisy intra-annual Mg/Ca patterns. Mg-enriched IOM associated with non-annual growth lines formed in response to other disturbances such as reproduction, temperature, or osmotic stress, may also complicate Mg/Ca profile interpretations. However, the intertidal, estuarine oysters used in this study likely experience a wider range of environmental

⁴ Note that because our analyses were performed on the resiliifer, the growth rate reflected in the $\delta^{18}\text{O}$ and Mg/Ca profiles is that of the resiliifer, and not necessarily that of the whole shell. A linear regression of resiliifer height against whole-valve height for 256 left valves from the modern South Carolina samples, however, shows the two dimensions are well correlated (whole shell height = $3.08 \times$ resiliifer height + 17.09; $R^2 = 0.75$; $F_{1,253} = 743.3$; $p \leq 0.0001$).

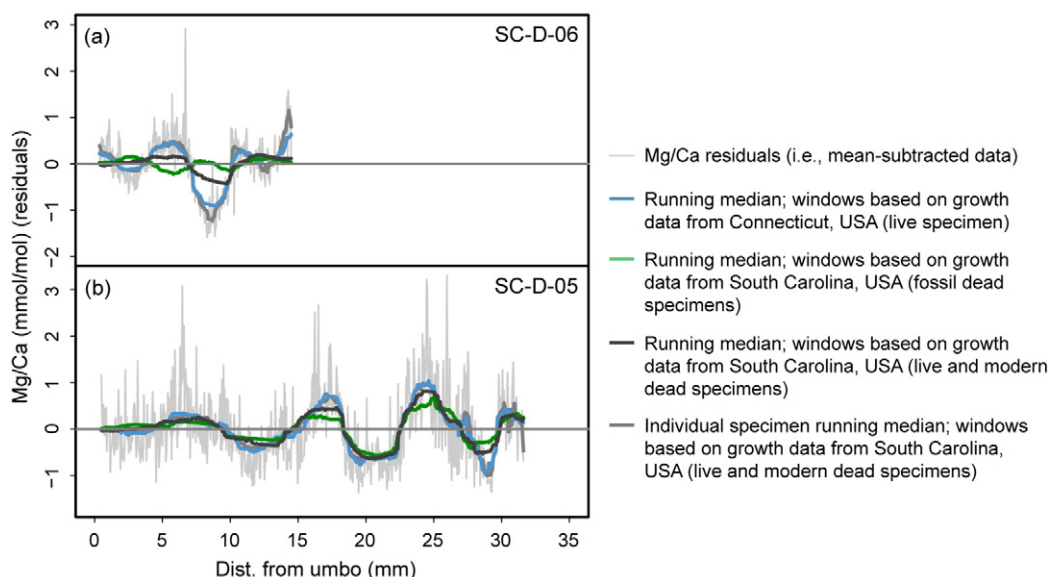


Fig. 6. Mg/Ca profiles for two modern *C. virginica* specimens from South Carolina: (a) SC-D-06 and (b) SC-D-05, demonstrating the decrease in the match between the running medians in smaller specimens (i.e., SC-D-06 in this case) because of the way the median window widths were calculated. See text for details.

stresses than mollusks living in full marine conditions, suggesting that this may not be a very common impediment to analyzing Mg/Ca profiles.

Salinity variations are another potential source of disagreement because Mg/Ca ratios have low sensitivity to salinity fluctuations above about 10 (Dodd and Crisp, 1982), but $\delta^{18}\text{O}$ and $\delta^{13}\text{C}$ values are typically both positively correlated with salinity (Epstein and Mayeda, 1953; Mook and Tan, 1991). Although *C. virginica* can survive salinities of 5 or lower for short periods, optimal salinities are typically 14–28 and populations inhabiting waters with average salinities around 10 tend to be sparse (Shumway, 1996), thus it is unlikely that the oysters used in our study—all of which were collected from areas with dense oyster populations—regularly experienced salinities below 10. Indeed, a regression of the $\delta^{18}\text{O}$ and $\delta^{13}\text{C}$ values measured from our specimens showed they were positively correlated overall ($\delta^{18}\text{O} = 0.61 * \delta^{13}\text{C} - 0.93$; $R^2 = 0.23$; $p \leq 0.0001$), and thus likely reflect salinity variations (cf. Gillikin et al., 2006) given the coastal marsh environments inhabited by *C. virginica* and *M. gigas* (see also Goodwin et al., 2010). We consider it unlikely that salinity variations influenced the match between the Mg/Ca and $\delta^{18}\text{O}$ profiles for most specimens, however, because there were few large excursions in the $\delta^{13}\text{C}$ profiles and there was generally a good correspondence between the Mg/Ca profiles and the $\delta^{18}\text{O}$ profiles. Two potential exceptions were specimens SC-L-01 and LA-D-01 (Figs. A3.2 and A3.16), both of which showed prominent, simultaneous, positive excursions in the $\delta^{18}\text{O}$ and $\delta^{13}\text{C}$ profiles that were not reflected in the Mg/Ca profiles (i.e., consistent with short-term increases in salinity).

Finally, Mg concentration has been shown to vary with distance from the edge of shell cross-sections in the calcitic bivalve *Pecten maximus* (Freitas et al., 2012). Specifically, Freitas et al. (2012) found that Mg/Ca ratios increased in magnitude and variability within ~200 μm of the exterior edge of the shell cross-section. Because the laser lines are straight but the shell layer in cross-section often is not (the reason multiple overlapping laser lines are required to construct the Mg/Ca profile), the distances from the laser lines to the exterior edges of the resiliifer cross-sections were not constant. For instance, laser lines frequently were <200 μm from the cross-section edge at the ends of line scans and in the resiliifer sections from early in ontogeny, when the foliated calcite layer is often very thin. We tested this relationship in *C. virginica* by regressing the distances of the laser lines from the edge of the cross-section against the variance in Mg/Ca values from the South Carolina *C. virginica* specimens (Appendix 4). Surprisingly, there

was a weak but statistically significant positive correlation between distance from the exterior edge of the cross-section and the mean (Mg/Ca mean = $0.73 * \text{Dist.} + 2.3$; $R^2 = 0.02$; $p = 0.0019$; Fig. A4.1) and variance (Mg/Ca variance = $0.31 * \text{Dist.} + 0.13$; $R^2 = 0.05$; $p \leq 0.0001$; Fig. A4.2) of Mg/Ca ratios, suggesting that the mean and variability of ratios increase with distance from the exterior edge of the resiliifer cross-section in *C. virginica* (Appendix 4), counter to previous findings in *Pecten*. These weak relationships, however, make it unlikely that the distance of the laser lines from the cross-section edge affected the Mg/Ca profile interpretations for the specimens in our study.

3.3. Advantages of Mg/Ca ratios over $\delta^{18}\text{O}$ values for sclerochronology

There are a few major potential advantages to choosing Mg/Ca-based sclerochronological analyses over stable isotope analyses for at least some applications, including the relative ease of higher resolution sampling that is possible with the LA-ICP-MS technique, as well as its lower time and financial costs. For instance, an interesting possibility is that the high-resolution sampling afforded by laser ablation line scans (~50 μm in this case, but LA-ICP-MS resolution can be easily adjusted by changing the laser scan rate and involves little additional sampling effort or cost) may out-perform $\delta^{18}\text{O}$ profiles for detecting some late-ontogeny annual cycles, because each LA-ICP-MS measurement is less time-averaged than the typical point samples milled for stable isotope analyses (resolution usually ~300 μm ; see Goodwin et al., 2003). A potential example of this advantage is specimen CT-L-01, the longest-lived specimen in our study. There is an additional trough and peak at the distal end of the Mg/Ca profile for CT-L-01, relative to the $\delta^{18}\text{O}$ profile, thus possibly capturing almost an additional year of growth missed by the $\delta^{18}\text{O}$ profile (Fig. 5). This example highlights the fact that although life-history trait estimates from $\delta^{18}\text{O}$ profiles are generally considered reliable, they are not always completely accurate or easily interpretable (e.g., Goodwin et al., 2003).

In addition, the lower time and financial costs of LA-ICP-MS relative to stable isotope analyses allow for more shells to be analyzed. The benefits of larger sample sizes may outweigh the costs associated with the occasionally challenging profile interpretations, particularly for life-history studies of populations. To illustrate this point, for the present study we completed stable isotope sampling for no more than three specimens per day and there was a turnaround time of at least one week to acquire the data, whereas we sampled up to ~10–15 specimens per day by LA-ICP-MS and the results were available in real time.

Finally, interpretation of $\delta^{18}\text{O}$ analyses of estuarine taxa, such as *C. virginica* and *M. gigas*, is sometimes challenging due to the combined influence of temperature and salinity on $\delta^{18}\text{O}$ water values (e.g., Surge et al., 2003). Thus, another potential advantage of using Mg/Ca profiles measured by LA-ICP-MS for characterizing mollusk shell growth characteristics is the low sensitivity of Mg/Ca ratios to salinity fluctuations relative to $\delta^{18}\text{O}$ values (Dodd and Crisp, 1982).

3.4. Conclusions

Our results suggest that Mg/Ca ratios measured from LA-ICP-MS line scans are a viable alternative to more traditional stable oxygen isotope analyses for estimating lifespans and growth rates of oysters and other mollusks that lack reliable annual morphological shell features. We also found that running medians with median windows based on shell growth data can capture annual cycles in the Mg/Ca profiles, making them easier to interpret. Further, plotting multiple running medians based on different sets of growth data or scaled to different maximum growth distances can aid the interpretation of ambiguous peaks and troughs in the Mg/Ca profiles. Although $\delta^{18}\text{O}$ profiles have been used extensively for sclerochronological applications for decades, the lower time and financial costs and increased sampling resolution of LA-ICP-MS analyses are potentially significant advantages over stable oxygen isotope analyses, particularly for studies requiring analysis of large numbers of specimens. Future research should further investigate the reasons for mismatches between the Mg/Ca and $\delta^{18}\text{O}$ profiles, particularly in ontogenetically early and late sections.

Acknowledgments

We thank A. Cohen for providing access to the *M. gigas* specimens from California, the Jarrett Bay Oyster Company (www.jarrettbayoysters.com) for supplying the hatchery reared *C. virginica* specimens from North Carolina, and Indian River Shellfish (www.indianrivershellfish.com) and the Madison Shellfish Commission for allowing us to collect *C. virginica* from Madison, Connecticut. We also thank J. Smith, A. Tweitmann, T. Butler, and M. Durham for assistance with fieldwork; A. Verheyden-Gillikin, M. Manon, S. Katz, and M. King for lab assistance at Union College; E. Mosier and C. Sweeney for lab assistance at Cornell University; and L. Ivany (Syracuse University) for micromill use. We also gratefully acknowledge funding support from the Atkinson Center for a Sustainable Future's Sustainable Biodiversity Fund (award to SRD) and the U.S. National Science Foundation for graduate research fellowship support to SRD (NSF-DGE #1144153). We also thank the U.S. National Science Foundation for providing funding for Union College's Perkin Elmer ICP-MS (NSF-CCLI #9952410), CETAC LSX-213 (NSF-MRI #1039832), and isotope ratio mass spectrometer and peripherals (NSF-MRI #1229258). Finally, we thank W. Allmon, M. Hare, J. Wehmiller, and I. Montanez (editor) for comments that helped improve the manuscript, as well as one anonymous reviewer, D. Surge, and S. Finnegan, for excellent reviews of the manuscript.

Supplementary data

Appendices 1–4 to this article can be found online at <http://dx.doi.org/10.1016/j.palaeo.2017.06.013>.

References

Andrus, C.F.T., 2011. Shell midden sclerochronology. *Quat. Sci. Rev.* 30:2892–2905. <http://dx.doi.org/10.1016/j.quascirev.2011.07.016>.

Andrus, C.F.T., Crowe, D.E., 2000. Geochemical analysis of *Crassostrea virginica* as a method to determine season of capture. *J. Archaeol. Sci.* 27, 33–42.

Baggett, L.P., Powers, S.P., Brumbaugh, R.D., Coen, L.D., DeAngelis, B.M., Greene, J.K., Hancock, B.T., Morlock, S.M., Allen, B.L., Breitburg, D.L., Bushek, D., Grabowski, J.H., Grizzle, R.E., Grosholz, E.D., La Peyre, M.K., Luckenbach, M.V., McGraw, K.A., Piehler, M.F., Westby, S.R., zu Ermgassen, P.S.E., 2015. Guidelines for evaluating performance

of oyster habitat restoration. *Restor. Ecol.* 23:737–745. <http://dx.doi.org/10.1111/rec.12262>.

Bougeois, L., de Raféllis, M., Reichart, G.-J., de Nooijer, L.J., Nicollin, F., Dupont-Nivet, G., 2014. A high resolution study of trace elements and stable isotopes in oyster shells to estimate Central Asian Middle Eocene seasonality. *Chem. Geol.* 363:200–212. <http://dx.doi.org/10.1016/j.chemgeo.2013.10.037>.

Bougeois, L., de Raféllis, M., Reichart, G.-J., de Nooijer, L.J., Dupont-Nivet, G., 2016. Mg/Ca in fossil oyster shells as palaeotemperature proxy, an example from the Palaeogene of Central Asia. *Palaeogeogr. Palaeoclimatol. Palaeoecol.* 441 (Part 4):611–626. <http://dx.doi.org/10.1016/j.palaeo.2015.09.052>.

Carriker, M.R., Gaffney, P.M., 1996. A catalogue of selected species of living oysters (Ostreacea) of the world. In: Kennedy, V.S., Newell, R.I.E., Eble, A.F. (Eds.), *The Eastern Oyster, Crassostrea virginica*. Maryland Sea Grant College, College Park, MD, pp. 1–18.

Cook, E.R., Holmes, R.L., 1986. User's manual for program ARSTAN. In: Holmes, R.L., Adams, R.K., Fritts, H.C. (Eds.), *Tree-ring Chronologies of Western North America: California, Eastern Oregon and Northern Great Basin with Procedures Used in the Chronology Development Work Including Users Manuals for Computer Programs COFECHA and ARSTAN*. University of Arizona, Tucson, AZ, Laboratory of Tree-Ring Research, pp. 50–65.

Cook, E.R., Krusic, P.J., 2005. ARSTAN v. 41d: A Tree-Ring Standardization Program Based on Detrending and Autoregressive Time Series Modeling, with Interactive Graphics. Tree-Ring Laboratory, Lamont-Doherty Earth Observatory of Columbia University, Palisades, New York, USA.

Cook, E.R., Peters, K., 1997. Calculating unbiased tree-ring indices for the study of climatic and environmental change. *The Holocene* 7, 361–370.

Custer, J.F., Doms, K.R., 1990. Analysis of microgrowth patterns of the American oyster (*Crassostrea virginica*) in the middle Atlantic region of eastern North America: archaeological applications. *J. Archeol. Sci.* 17:151–160. [http://dx.doi.org/10.1016/0305-4403\(90\)90056-B](http://dx.doi.org/10.1016/0305-4403(90)90056-B).

Dodd, J.R., 1965. Environmental control of strontium and magnesium in *Mytilus*. *Geochim. Cosmochim. Acta* 29, 385–398.

Dodd, J.R., Crisp, E.L., 1982. Non-linear variation with salinity of Sr/Ca and Mg/Ca ratios in water and aragonitic bivalve shells and implications for paleosalinity studies. *Palaeogeogr. Palaeoclimatol. Palaeoecol.* 38, 45–56.

Durrant, S.F., Ward, N.I., 2005. Recent biological and environmental applications of laser ablation inductively coupled plasma mass spectrometry (LA-ICP-MS). *J. Anal. At. Spectrom.* 20:821–829. <http://dx.doi.org/10.1039/B502206A>.

Epstein, S., Mayeda, T., 1953. Variation of O^{18} content of waters from natural sources. *Geochim. Cosmochim. Acta* 4:213–224. [http://dx.doi.org/10.1016/0016-7037\(53\)90051-9](http://dx.doi.org/10.1016/0016-7037(53)90051-9).

Fabre, C., Lathuilière, B., 2007. Relationships between growth-bands and paleoenvironmental proxies Sr/Ca and Mg/Ca in hypercalcified sponge: a micro-laser induced breakdown spectroscopy approach. *Spectrochim. Acta B At. Spectrosc.* 62:1537–1545. <http://dx.doi.org/10.1016/j.sab.2007.10.045>.

Fan, C., Koeniger, P., Wang, H., Frechen, M., 2011. Ligamental increments of the mid-Holocene Pacific oyster *Crassostrea gigas* are reliable independent proxies for seasonality in the western Bohai Sea, China. *Palaeogeogr. Palaeoclimatol. Palaeoecol.* 299: 437–448. <http://dx.doi.org/10.1016/j.palaeo.2010.11.022>.

Foster, L.C., Finch, A.A., Allison, N., Andersson, C., Clarke, L.J., 2008. Mg in aragonitic bivalve shells: seasonal variations and mode of incorporation in *Arctica islandica*. *Chem. Geol.* 254:113–119. <http://dx.doi.org/10.1016/j.chemgeo.2008.06.007>.

Freitas, P.S., Clarke, L.J., Kennedy, H., Richardson, C.A., 2012. The potential of combined Mg/Ca and $\delta^{18}\text{O}$ measurements within the shell of the bivalve *Pecten maximus* to estimate seawater $\delta^{18}\text{O}$ composition. *Chem. Geol.* 291:286–293. <http://dx.doi.org/10.1016/j.chemgeo.2011.10.023>.

Gillikin, D.P., Lorrain, A., Bouillon, S., Willenz, P., Dehairs, F., 2006. Stable carbon isotopic composition of *Mytilus edulis* shells: relation to metabolism, salinity, $\delta^{13}\text{C}_{\text{DIC}}$ and phytoplankton. *Org. Geochem.* 37:1371–1382. <http://dx.doi.org/10.1016/j.orggeochem.2006.03.008>.

Goodwin, D.H., Schöne, B.R., Dettman, D.L., 2003. Resolution and fidelity of oxygen isotopes as paleotemperature proxies in bivalve mollusk shells: models and observations. *PALAIOS* 18, 110–125.

Goodwin, D.H., Cohen, A.N., Roopnarine, P.D., 2010. Forensics on the half shell: a sclerochronological investigation of a modern biological invasion in San Francisco Bay, United States. *PALAIOS* 25:742–753. <http://dx.doi.org/10.2110/palo.2010.p10-015r>.

Goodwin, D.H., Gillikin, D.P., Roopnarine, P.D., 2013. Preliminary evaluation of potential stable isotope and trace element productivity proxies in the oyster *Crassostrea gigas*. *Palaeogeogr. Palaeoclimatol. Palaeoecol.* 373:88–97. <http://dx.doi.org/10.1016/j.palaeo.2012.03.034>.

Graniero, L.E., Surge, D., Gillikin, D.P., Briz, I., Godino, I., Álvarez, M., 2017. Assessing elemental ratios as a paleotemperature proxy in the calcite shells of patelloid limpets. *Palaeogeogr. Palaeoclimatol. Palaeoecol.* 465:376–385. <http://dx.doi.org/10.1016/j.palaeo.2016.10.021>.

Gröcke, D.R., Gillikin, D.P., 2008. Advances in mollusk sclerochronology and sclerochemistry: tools for understanding climate and environment. *Geo-Mar. Lett.* 28:265–268. <http://dx.doi.org/10.1007/s00367-008-0108-4>.

Harding, J.M., Mann, R., Southworth, M.J., Wesson, J.A., 2010. Management of the Piankank River, Virginia, in support of oyster (*Crassostrea virginica*, Gmelin 1791) fishery repletion. *J. Shellfish Res.* 29, 867–888.

Hong, W., Keppens, E., Nielsen, P., van Riet, A., 1995. Oxygen and carbon isotope study of the Holocene oyster reefs and paleoenvironmental reconstruction on the northwest coast of Bohai Bay, China. *Mar. Geol.* 124:289–302. [http://dx.doi.org/10.1016/0025-3227\(95\)00046-2](http://dx.doi.org/10.1016/0025-3227(95)00046-2).

Johnson, A.L.A., Liquorish, M.N., Sha, J., 2007. Variation in growth-rate and form of a Bathonian (Middle Jurassic) oyster in England, and its environmental implications. *Palaeontology* 50:1155–1173. <http://dx.doi.org/10.1111/j.1475-4983.2007.00698.x>.

- Jones, D.S., Arthur, M.A., Allard, D.J., 1989. Sclerochronological records of temperature and growth from shells of *Mercenaria mercenaria* from Narragansett Bay, Rhode Island. *Mar. Biol.* 102, 225–234.
- Kirby, M.X., 2001. Differences in growth rate and environment between Tertiary and Quaternary *Crassostrea* oysters. *Paleobiology* 27:84–103. [http://dx.doi.org/10.1666/0094-8373\(2001\)027<0084:DIGRAE>2.0.CO;2](http://dx.doi.org/10.1666/0094-8373(2001)027<0084:DIGRAE>2.0.CO;2).
- Kirby, M.X., Soniat, T.M., Spero, H.J., 1998. Stable isotope sclerochronology of Pleistocene and Recent oyster shells (*Crassostrea virginica*). *PALAIOS* 13:560–569. <http://dx.doi.org/10.2307/3515347>.
- Klein, R.T., Lohmann, K.C., Thayer, C.W., 1996. Bivalve skeletons record sea-surface temperature and $\delta^{18}\text{O}$ via Mg/Ca and $^{18}\text{O}/^{16}\text{O}$ ratios. *Geology* 24, 415–418.
- Kraeuter, J.N., Ford, S., Cummings, M., 2007. Oyster growth analysis: a comparison of methods. *J. Shellfish Res.* 26:479–491. [http://dx.doi.org/10.2983/0730-8000\(2007\)26\[479:OGAAO\]2.0.CO;2](http://dx.doi.org/10.2983/0730-8000(2007)26[479:OGAAO]2.0.CO;2).
- Langlet, D., Alunno-Bruscia, M., Rafélis, M., Renard, M., Roux, M., Schein, E., Buestel, D., 2006. Experimental and natural cathodoluminescence in the shell of *Crassostrea gigas* from Thau lagoon (France): ecological and environmental implications. *Mar. Ecol. Prog. Ser.* 317, 143–156.
- Lartaud, F., de Rafélis, M., Ropert, M., Emmanuel, L., Geairon, P., Renard, M., 2010. Mn labelling of living oysters: artificial and natural cathodoluminescence analyses as a tool for age and growth rate determination of *C. gigas* (Thunberg, 1793) shells. *Aquaculture* 300:206–217. <http://dx.doi.org/10.1016/j.aquaculture.2009.12.018>.
- Levinton, J., Doall, M., Allam, B., 2013. Growth and mortality patterns of the eastern oyster *Crassostrea virginica* in impacted waters in coastal waters in New York, USA. *J. Shellfish Res.* 32:417–427. <http://dx.doi.org/10.2983/035.032.0222>.
- Lorrain, A., Gillikin, D.P., Paulet, Y.-M., Chauvaud, L., Mercier, A.L., Navez, J., André, L., 2005. Strong kinetic effects on Sr/Ca ratios in the calcitic bivalve *Pecten maximus*. *Geology* 33:965–968. <http://dx.doi.org/10.1130/G22048.1>.
- Mann, R., Harding, J.M., Southworth, M.J., 2009. Reconstructing pre-colonial oyster demographics in the Chesapeake Bay, USA. *Estuar. Coast. Shelf Sci.* 85:217–222. <http://dx.doi.org/10.1016/j.ecss.2009.08.004>.
- Marali, S., Schöne, B.R., Mertz-Kraus, R., Griffin, S.M., Wanamaker Jr., A.D., Butler, P.G., Holland, H.A., Jochum, K.P., 2017. Reproducibility of trace element time-series (Na/Ca, Mg/Ca, Mn/Ca, Sr/Ca, and Ba/Ca) within and between specimens of the bivalve *Arctica islandica* – A LA-ICP-MS line scan study. *Palaeogeogr. Palaeoclimatol. Palaeoecol.* 484, 109–128.
- Mook, W.G., Tan, F.C., 1991. Stable carbon isotopes in rivers and estuaries. In: Degens, E.T., Kempe, S., Richey, J.E. (Eds.), *Biogeochemistry of Major World Rivers*. SCOPE Series. John Wiley & Sons Ltd, New York, pp. 245–264.
- Mouchi, V., de Rafélis, M., Lartaud, F., Fialin, M., Verrecchia, E., 2013. Chemical labelling of oyster shells used for time-calibrated high-resolution Mg/Ca ratios: a tool for estimation of past seasonal temperature variations. *Palaeogeogr. Palaeoclimatol. Palaeoecol.* 373:66–74. <http://dx.doi.org/10.1016/j.palaeo.2012.05.023>.
- O'Neil, D.D., Gillikin, D.P., 2014. Do freshwater mussel shells record road salt pollution? *Sci Rep* 4:7168. <http://dx.doi.org/10.1038/srep07168>.
- Oomori, T., Kaneshima, H., Maezato, Y., Kitano, Y., 1987. Distribution coefficient of Mg^{2+} ions between calcite and solution at 10–50 °C. *Mar. Chem.* 20:327–336. [http://dx.doi.org/10.1016/0304-4203\(87\)90066-1](http://dx.doi.org/10.1016/0304-4203(87)90066-1).
- Pearce, N.J.G., Perkins, W.T., Westgate, J.A., Gorton, M.P., Jackson, S.E., Neal, C.R., Chenery, S.P., 1997. A compilation of new and published major and trace element data for NIST SRM 610 and NIST SRM 612 glass reference materials. *Geostand. Newslett.* 21: 115–144. <http://dx.doi.org/10.1111/j.1751-908X.1997.tb00538.x>.
- Poulain, C., Gillikin, D.P., Thébault, J., Munaron, J.M., Bohn, M., Robert, R., Paulet, Y.-M., Lorrain, A., 2015. An evaluation of Mg/Ca, Sr/Ca, and Ba/Ca ratios as environmental proxies in aragonite bivalve shells. *Chem. Geol.* 396:42–50. <http://dx.doi.org/10.1016/j.chemgeo.2014.12.019>.
- Rasband, W.S., 1997. ImageJ. U. S. National Institutes of Health, Bethesda, Maryland, USA.
- Richardson, C.A., Collis, S.A., Ekaratne, K., Dare, P., Key, D., 1993. The age determination and growth rate of the European flat oyster, *Ostrea edulis*, in British waters determined from acetate peels of umbo growth lines. *ICES J. Mar. Sci. J. Cons.* 50: 493–500. <http://dx.doi.org/10.1006/jmsc.1993.1052>.
- Richardson, C.A., Peharda, M., Kennedy, H., Kennedy, P., Onofri, V., 2004. Age, growth rate and season of recruitment of *Pinna nobilis* (L) in the Croatian Adriatic determined from Mg:Ca and Sr:Ca shell profiles. *J. Exp. Mar. Biol. Ecol.* 299:1–16. <http://dx.doi.org/10.1016/j.jembe.2003.08.012>.
- Richardson, C.A., Saurel, C., Barroso, C.M., Thain, J., 2005. Evaluation of the age of the red whelk *Neptunea antiqua* using statoliths, opercula and element ratios in the shell. *J. Exp. Mar. Biol. Ecol.* 325:55–64. <http://dx.doi.org/10.1016/j.jembe.2005.04.024>.
- Rick, T.C., Reeder-Myers, L.A., Hofman, C.A., Breitburg, D., Lockwood, R., Henkes, G., Kellogg, L., Lowery, D., Luckenbach, M.W., Mann, R., Ogburn, M.B., Southworth, M., Wah, J., Wesson, J., Hines, A.H., 2016. Millennial-scale sustainability of the Chesapeake Bay Native American oyster fishery. *Proc. Natl. Acad. Sci.* 201600019. <http://dx.doi.org/10.1073/pnas.1600019113>.
- Salvi, D., Mariottini, P., 2016. Molecular taxonomy in 2D: a novel ITS2 rRNA sequence-structure approach guides the description of the oysters' subfamily Saccostreinae and the genus *Magallana* (Bivalvia: Ostreidae). *Zool. J. Linnean Soc.* <http://dx.doi.org/10.1111/zoj.12455> (13 pp.).
- Savarese, M., Walker, K.J., Stingu, S., Marquardt, W.H., Thompson, V., 2016. The effects of shellfish harvesting by aboriginal inhabitants of Southwest Florida (USA) on productivity of the eastern oyster: implications for estuarine management and restoration. *Anthropocene* 16:28–41. <http://dx.doi.org/10.1016/j.ancene.2016.10.002>.
- Schöne, B.R., Zhang, Z., Jacob, D., Gillikin, D.P., Tütken, T., Garbe-Schönberg, D., McConnaughey, T., Soldati, A., 2010. Effect of organic matrices on the determination of the trace element chemistry (Mg, Sr, Mg/Ca, Sr/Ca) of aragonitic bivalve shells (*Arctica islandica*)—comparison of ICP-OES and LA-ICP-MS data. *Geochem. J.* 44, 23–37.
- Schöne, B.R., Zhang, Z., Radermacher, P., Thébault, J., Jacob, D.E., Nunn, E.V., Maurer, A.-F., 2011. Sr/Ca and Mg/Ca ratios of ontogenetically old, long-lived bivalve shells (*Arctica islandica*) and their function as paleotemperature proxies. *Palaeogeogr. Palaeoclimatol. Palaeoecol.* 302:52–64. <http://dx.doi.org/10.1016/j.palaeo.2010.03.016>.
- Sherwood, O.A., Heikoop, J.M., Sinclair, D.J., Scott, D.B., Risk, M.J., Shearer, C., Azetsu-Scott, K., 2005. Skeletal Mg/Ca in *Primnoa resedaeformis*: relationship to temperature? In: Freiwald, A., Roberts, J.M. (Eds.), *Cold-Water Corals and Ecosystems*. Springer, Berlin Heidelberg, New York, pp. 1061–1079.
- Shumway, S.E., 1996. Natural environmental factors. In: Kennedy, V.S., Newell, R.I.E., Eble, A.F. (Eds.), *The Eastern Oyster, Crassostrea virginica*. Maryland Sea Grant College, College Park, MD, pp. 467–513.
- Spalding, M.D., Fox, H.E., Allen, G.R., Davidson, N., Ferdaña, Z.A., Finlayson, M.A.X., Halpern, B.S., Jorge, M.A., Lombana, A.L., Lourie, S.A., et al., 2007. Marine ecoregions of the world: a bioregionalization of coastal and shelf areas. *Bioscience* 57, 573–583.
- Surge, D., Lohmann, K.C., 2008. Evaluating Mg/Ca ratios as a temperature proxy in the estuarine oyster, *Crassostrea virginica*. *J. Geophys. Res. Biogeosci.* 113, G02001. <http://dx.doi.org/10.1029/2007JG000623>.
- Surge, D., Lohmann, K.C., Dettman, D.L., 2001. Controls on isotopic chemistry of the American oyster, *Crassostrea virginica*: implications for growth patterns. *Palaeogeogr. Palaeoclimatol. Palaeoecol.* 172, 283–296.
- Surge, D.M., Lohmann, K.C., Goodfriend, G.A., 2003. Reconstructing estuarine conditions: oyster shells as recorders of environmental change, Southwest Florida. *Estuar. Coast. Shelf Sci.* 57:737–756. [http://dx.doi.org/10.1016/S0272-7714\(02\)00370-0](http://dx.doi.org/10.1016/S0272-7714(02)00370-0).
- Swart, P.K., Thorrold, S., Rosenheim, B., Eisenhauer, A., Harrison, C.G.A., Grammer, M., Latkoczy, C., 2002. Intra-annual variation in the stable oxygen and carbon and trace element composition of sclerosponges. *Paleoceanography* 17:1045. <http://dx.doi.org/10.1029/2000PA000622>.
- Takesue, R.K., van Geen, A., 2004. Mg/Ca, Sr/Ca, and stable isotopes in modern and Holocene *Protothaca staminea* shells from a northern California coastal upwelling region. *Geochim. Cosmochim. Acta* 68:3845–3861. <http://dx.doi.org/10.1016/j.gca.2004.03.021>.
- Thomas, K.D., 2015. Molluscs emergent, part I: themes and trends in the scientific investigation of mollusc shells as resources for archaeological research. *J. Archaeol. Sci.* 56: 133–140. <http://dx.doi.org/10.1016/j.jas.2015.01.024>.
- Twaddle, R.W., Ulm, S., Hinton, J., Wurster, C.M., Bird, M.I., 2016. Sclerochronological analysis of archaeological mollusc assemblages: methods, applications and future prospects. *Archaeol. Anthropol. Sci.* 8:359–379. <http://dx.doi.org/10.1007/s12520-015-0228-5>.
- Tynan, S., Opdyke, B.N., Walczak, M., Eggins, S., Dutton, A., 2017. Assessment of Mg/Ca in *Saccostrea glomerata* (the Sydney rock oyster) shell as a potential temperature record. *Palaeogeogr. Palaeoclimatol. Palaeoecol.* 484, 79–88.
- USGS, 2012. United States Geological Survey Preliminary Certificate of Analysis, Microanalytical Carbonate Standard, MACS-3 (2pp).
- Vander Putten, E., Dehairs, F., André, L., Baeyens, W., 1999. Quantitative in situ microanalysis of minor and trace elements in biogenic calcite using infrared laser ablation-inductively coupled plasma mass spectrometry: a critical evaluation. *Anal. Chim. Acta* 378, 261–272.
- Wanamaker Jr., A.D., Kreutz, K.J., Wilson, T., Borns Jr., H.W., Introne, D.S., Feindel, S., 2008. Experimentally determined Mg/Ca and Sr/Ca ratios in juvenile bivalve calcite for *Mytilus edulis*: implications for paleotemperature reconstructions. *Geo-Mar. Lett.* 28:359–368. <http://dx.doi.org/10.1007/s00367-008-0112-8>.
- Watanabe, T., Winter, A., Oba, T., 2001. Seasonal changes in sea surface temperature and salinity during the Little Ice Age in the Caribbean Sea deduced from Mg/Ca and $^{18}\text{O}/^{16}\text{O}$ ratios in corals. *Mar. Geol.* 173:21–35. [http://dx.doi.org/10.1016/S0025-3227\(00\)00166-3](http://dx.doi.org/10.1016/S0025-3227(00)00166-3).
- Wehmiller, J.F., Belknap, D.F., Boutin, B.S., Mirecki, J.E., Rahaim, S.D., York, L.L., 1988. A review of the aminostratigraphy of Quaternary mollusks from United States Atlantic Coastal Plain sites. *Geol. Soc. Am. Spec. Pap.* 227:69–110. <http://dx.doi.org/10.1130/SPE227-p69>.